Interplay between silicate and hydroxide ions during geopolymerization

J. Aupoil, J.-B. Champenois, J.-B. d'Espinose de Lacaillerie, A. Poulesquen

Interplay between silicate and hydroxide ions during geopolymerization

Julien Aupoil[1,2], *Jean-Baptiste Champenois*[1,*], *Jean-Baptiste d'Espinose de Lacaillerie*[2], *Arnaud Poulesquen*[1]

[1]CEA, DEN, DE2D, SEAD, LCBC, F-30207 Bagnols-sur-Cèze, France

[2]Laboratoire de Sciences et Ingénierie de la Matière Molle, UMR CNRS 7615, ESPCI Paris, PSL Research University, 10, rue Vauquelin, 75231 Paris Cedex 05, France

[*] Corresponding author

Keywords: silicate, hydroxide, Hammet, alkali, metakaolin, dissolution, condensation,

Abstract

Two set of activating solutions were prepared with increasing sodium hydroxide content, either containing or not silicates. Their alkalinities, here defined as the ability of solutions to resist changes in pH, were determined and compared by measuring Hammet acidity functions that can be assimilated to extended pH values. Such Hammet functions in sodium silicate solutions are reported for the first time. The impact of both the alkalinity and the initial Hammett function on the reactivity of metakaolin (MK)-based pastes was assessed using Isothermal Conduction micro-Calorimetry (ICC). It was concluded that the reactivity of MK mixed with sodium hydroxide solution related directly to the Hammett function values whereas in sodium silicate mixes, the alkalinity value was a more pertinent parameter. A mechanism was deduced to clarify the role of hydroxide ions during the geopolymerization, highlighting at the same time the role of silicate species as hydroxide reservoir to nurture the dissolution process.

1. Introduction

Geopolymers refer to alumino-silicate binders obtained by reaction of a powdered alumino-silicate source, such as dehydroxylated kaolin (metakaolin, MK), with an alkali hydroxide or alkali silicate solution, as described by Davidovits[1]. Schematically, the geopolymerization process can be described by three simplified steps[2-5]. First, MK dissolution in the activating solution provides aluminate and silicate species to the reacting medium. These species then rearrange in solution, to finally polycondense, yielding the 3D network of the hardened geopolymer.

Carrying out a detailed mechanistic study of these three steps is a hard task. They occur concurrently and furthermore, no realistic reaction equations can be written to describe any of these steps. However, since most of the expected reaction steps are exothermic, the use of Isothermal Conduction Calorimetry (ICC) was previously reported[6-11] as being an efficient tool for studying the whole geopolymerization process. Indeed, heat flow and heat profiles recorded during geopolymerization provide qualitative and quantitative information. As an example, the global geopolymerization extent at a given time has been calculated as the ratio of the cumulated heat Q(t) release to the theoretical total heat at completion, Q_{max}[6,9,10]. Hence, in alkali hydroxide activating solutions free from silicates, Zhang *et al.*[9] reported an increase of the aforementioned geopolymerization extent with increasing hydroxide ions content.

The relationship between activating solution composition and geopolymerization has been the subject of an extensive body of literature. Indeed, such a topic is a key issue for the use of geopolymers and their industrial development. For examples, Rahier *et al.*[12] reported that the activating solution modulus, defined as the SiO_2/Na_2O molar ratio, and the amount of water, defined as the H_2O/Na_2O molar ratio, are driving parameters to tune geopolymers stoichiometry

and consistency respectively. At a Na/Al molar ratio equal to one, the optimal geopolymer stoichiometry can thus be reached by choosing the appropriate SiO_2/Na_2O modulus of the activating solution. Later, Duxson *et al.*[13] observed an increase in the proportion of unreacted metakaolin and a decrease in the geopolymers density when increasing the silicate content of activating solutions as a consequence of the resulting simultaneous increase of the SiO_2/Al_2O_3 and SiO_2/Na_2O molar ratios. Such a result was further rationalized by using Density Functional Theory (DFT)-based Coarse-Grain Monte-Carlo simulations[14]. Similarly, Zhang *et al.*[10] reported that an increase in the activating solution modulus, defined as the SiO_2/Na_2O molar ratio, leads to a decrease in the geopolymerization extent, evaluated by isothermal calorimetry.

The use of ^{29}Si Nuclear Magnetic Resonance (NMR) clearly exhibited that silicates connectivity in activating solutions increases when increasing the modulus of the solutions[15-17]. Duxson *et al.*[13] postulated that the higher the silicates connectivity, the lower the silicates species lability. According to these authors, highly connected silicate species would thus hardly rearrange and densify before gelation, leading to the formation of a gel of lesser density and thiner pore size distribution, around metakaolin grains.

In most of the aforementioned studies, the activating solutions compositions are described in terms of silicate content, SiO_2/Na_2O and H_2O/Na_2O molar ratios. The influence of the free hydroxide ions content on the geopolymerization reaction is thus not explicit. Although it had already been mentioned by Xu and Van Deventer[18] and Zhang *et al*[9], to the best of our knowledge, only one scientific paper has been dedicated to that topic. Indeed, by increasing the alkali hydroxide content of activating solutions and using fly ash as an aluminosilicate source, Phair and Van Deventer[19] reported that a higher activating solution pH leads to a higher

71 polycondensation extent. However, pH reported values seem to be approximate as they are given
72 only in full pH units[19]. In any case, these three studies[9,18,19] clearly highlight the importance of
73 hydroxide ions in the geopolymerization process.
74 An effect of solution pH on aluminosilicates dissolution was indeed evidenced by Xu and Van
75 Deventer[18] when studying in diluted suspensions the dissolution of 15 aluminosilicates minerals.
76 They concluded that the extent of dissolution increases for increasing alkali hydroxide solution
77 concentrations. Complementarily, Duxson *et al.*[2] (and references therein) and Granizo *et al.*[20]
78 amongst others also pinpointed that the dissolution kinetics of aluminosilicate sources was highly
79 dependent on the initial pH of the solution.
80 However, all the previously mentioned experiments[2,18,20] were carried out using solutions free
81 from silicates and using high liquid to solid ratio. As such, the role of silicate species and their
82 interplay with hydroxide ions on the dissolution step during geopolymerization have never been
83 investigated. This literature gap may have resulted from the difficulty to assess by standard pH-
84 metry pH values of solutions containing extremely high amounts of alkali metal ions.
85
86 In consequence, the present study firstly aims at quantifying the hydroxide content and the
87 alkalinity of two sets of activating solutions. Two sets of solutions of increasing sodium
88 hydroxide content were considered: the first one with a fixed silicate content and the second one
89 devoid of silicate species. Each time, Hammet acidity functions of studied solutions were
90 measured instead of pH, as described in the theoretical part. The corresponding alkalinity[21],
91 defined here as the ability of a solution to resist to changes in pH, was evaluated for the two sets
92 of solutions. Then, the geopolymers reactivity observed by mixing metakaolin into these
93 solutions was evaluated by using Isothermal Conduction Calorimetry (ICC). Finally, these new

94 data led us to discuss the role of silicate species and their interplay with hydroxide ions during
95 geopolymerization.
96

2. Theoretical basis.

In activating solutions used for geopolymers elaboration, molality of alkali metal ions can range between 1 mol / kg of water to 15 mol / kg of water. The use of a glass electrode sensitive to oxonium ions H_3O^+ to assess pH values is then questionable in such media. First, a high sodium concentration in basic solutions often leads to an alkaline error, since the alkali ion concentration can be typically orders of magnitudes larger than the oxonium ions one. As an example, the alkali ion concentration is 10^{14} times higher than the oxonium one in a sodium silicate solution containing 10 mol / kg of sodium ions at pH ≈ 13. Then, water activity in the studied solution can be far below the value of 0.9 expected in a 3 mol / kg potassium chloride electrode filling solution. As a consequence, the ionic flow from the electrode to the studied medium could be strongly impacted, leading to false measurements. Finally, in the specific case of silicate-containing activating solutions, silicate species can interact or even deteriorate the glass electrode surface, leading to additional errors.

Consequently, in this work, the measurement of Hammet acidity functions[22-24] was chosen instead of standard pH-metry to quantify the amount of hydroxide ions in activating solutions. Such a function represents the hydroxide ions ability to deprotonate a weak acid, noted SH in reaction equation 1, added in small amounts in the aqueous medium. It is obviously equivalent to pH in dilute systems. Upon introduction in the studied medium, again in small amounts, the weak acid SH plays the role of an acid-base indicator whose ionization ratio is measured quantitatively thanks to the intensity shift of its UV-visible spectrum induced by its deprotonation . This concept was initially introduced to measure acidity of extremely acidic solution and later adapted to basic solutions, either in aqueous alkali hydroxide solutions or in non-aqueous solvents[25-30].

120

121 $SH.xH_2O + OH^-.yH_2O = S^-.zH_2O + (n+1)H_2O$ (Reaction Equation 1)

122

123 In reaction equation 1, the coefficient $n = (x + y - z)$ accounts for the difference in hydration
124 degrees between reactants and products, according to the model used by Edward[29]. The
125 corresponding equilibrium constant K is then written as:

126 $$K = \frac{a_{S-} \cdot a_{H2O}^{(n+1)}}{a_{SH} \cdot a_{OH-}} = \frac{K_a}{K_w}$$ (Equation 1)

127 with a_i the activity of the species i.

128 As reaction equation 1 represents an acid-base reaction between the two couples SH/S^- and
129 OH^-/H_2O, the constant K can also be written as the ratio of the associated ionization constants: K_a
130 for the acid ionization constant of SH and K_w for the one of water (tabulated by Bandura and
131 Lvov[31] and taken as 10^{-14} at 25°C),

132 Hammett[23] defined the acidity function H_- according to equation 2. Rearranging equation 1 also
133 provides equation 3, another definition of the acidity function:

134 $$H_- = pK_a + log\frac{[S^-]}{[SH]}$$ (Equation 2)

135 $$H_- = pK_w + log\, a_{OH-} - (n+1).log\, a_{H2O} + log\frac{\gamma_{SH}}{\gamma_{S-}}$$ (Equation 3)

136 With:

137 pK_x the cologarithm of constant K_x,

138 $\frac{[S-]}{[SH]}$ the ionization ratio,

139 $[i]$ the concentration of species i in mol / kg of water,

140 and γ_i its activity coefficient defined such as $a_i = \gamma_i.[i]/[i]°$ where $[i]°$ is the standard state
141 concentration of species i conventionally set equal to 1 mol / kg.

The experimental determination of activity coefficients being complex, equation 3 is mainly of theoretical interest, except in the rare cases when good approximations of activity coefficients[24,29] are possible. Nevertheless, equation 3 clearly states that the function H_- takes into account not only the hydroxide ions activity but also their environment through the parameter n and the variables a_{H2O} and γ_{SH}/γ_{S^-}, respectively related to the ions hydration, the free water content and the ionic force of the solution. In consequence, the acidity function is an appropriate tool to represent the ability of hydroxide ions to react in a solution.

If both S^- and SH forms absorb UV-visible light at different wavelengths, the *[S-]/[SH]* ionization ratio can be measured by using spectrocolorimetry. From Beer-Lambert's law, the ionization ratio can be obtained from absorbance measurements for a constant indicator concentration according to (eq. 4).

$$\frac{[S^-]}{[SH]} = \frac{A - A_{SH}}{A_{S^-} - A} \qquad \text{(Equation 4)}$$

With

A_{SH} the absorbance of a solution where the indicator is fully protonated,

A_{S^-} the absorbance of a solution where the indicator is fully deprotonated,

A the absorbance of any basic solution with intermediate concentration.

A set of three solutions is thus needed to determine an ionization ratio.

3. Experimental section.

3.1. Activating solutions elaboration

Sodium hydroxide solutions were elaborated with an increasing molality ranging from $3.17 .10^{-2}$ to $1.40 .10^{1}$ mol / kg by dissolving sodium hydroxide pellets (AR grade, VWR) in ultrapure water (18.2 MΩ). A set of alkali silicate solutions was then elaborated by diluting in water a commercial alkali silicate solution (Betol® 52T, Wöllner: 30.2% w/w SiO_2, 14.7% w/w Na_2O and 55.1% w/w H_2O) and by adding sodium hydroxide pellets in order to reach increasing sodium ions molality, ranging from 5.46 to $1.40 .10^{1}$ mol/kg. All solutions were stirred for at least 4 h and cooled down to 25°C prior to any use. Solutions compositions are reported in Tables 1 and 2.

Table 1. Composition in molality, water activity and acidity function values of sodium hydroxide solutions together with the molar ratios of the corresponding geopolymers prepared with metakaolin. Acidity functions were taken from literature when indicated ([a] Rochester[32], [b] Schwarzenbach[25]).

	Solutions			Geopolymers	
	[NaOH] (mol/kg)	a_{H2O} (± 0.008)	H_-	Na/Al	$\frac{SiO_2}{Na_2O}$
Na1	$3.17 .10^{-2}$	1.000	12.51 ± 0.06	$3.28 .10^{-3}$	733
Na2	$1.00 .10^{-1}$	1.000	12.99 ± 0.06	$1.04 .10^{-2}$	232
Na3	$3.17 .10^{-1}$	-	13.42 ± 0.08	$3.28 .10^{-2}$	73.2
Na4	1.00	0.987	14.01[a]	$1.04 .10^{-1}$	23.2
Na5	2.00	0.956	14.42[a]	$2.07 .10^{-1}$	11.6
Na6	3.01	0.917	14.72[a]	$3.11 .10^{-1}$	7.73
Na7	5.00	0.812	15.19[a]	$5.18 .10^{-1}$	4.64
Na8	7.00	0.692	15.62[a]	$7.25 .10^{-1}$	3.32
Na9	9.66	0.520	16.06[a]	1.00	2.41
Na10	$1.20 .10^{1}$	-	16.47[b]	1.24	1.94
Na11	$1.40 .10^{1}$	0.275	16.87[b]	1.45	1.66

Table 2. Molality, molar ratio, water activity and acidity function values of sodium silicate solutions. When indicated, the composition of the corresponding geopolymers prepared with metakaolin is also given.

	Solutions						Geopolymers	
	$[NaOH]_{added}$ (mol/kg)	$[Na]_{total}$ (mol/kg)	[Si] (mol/kg)	$\frac{SiO_2}{Na_2O}$	a_{H2O} (± 0.008)	H_-	Na/Al	$\frac{SiO_2}{Na_2O}$
NaS1	0	5.46	5.79	2.12	0.965	-	0.57	6.36
NaS2	$5.26 .10^{-1}$	6.01	5.80	1.93	0.952	10.82 ± 1.98	0.62	5.79
NaS3	1.54	7.01	5.80	1.65	0.928	11.64 ± 0.35	0.73	4.97
NaS4	2.54	8.02	5.79	1.45	0.903	12.19 ± 0.14	0.83	4.34
NaS5	3.53	9.00	5.80	1.29	-	12.52 ± 0.10	-	-
NaS6	4.20	9.68	5.80	1.20	0.837	12.74 ± 0.10	1.00	3.60
NaS7	5.02	10.5	5.80	1.10	-	13.10 ± 0.11	-	-
NaS8	5.52	11.0	5.80	1.05	0.767	13.25 ± 0.12	1.14	3.16
NaS9	6.54	12.0	5.80	$9.66 .10^{-1}$	0.711	13.59 ± 0.20	1.24	2.68
NaS10	7.54	13.0	5.79	$8.91 .10^{-1}$	0.649	14.12 ± 0.53	1.34	2.32
NaS11	8.54	14.0	5.80	$8.27 .10^{-1}$	-	-	-	-

3.2. Geopolymers preparation

Prior to the cure and any measurements, geopolymer pastes were prepared by mixing 32.05 g of metakaolin (MK, Metakaolin Argical M1000 from Imerys, characteristics in Table 3) with the appropriate weight of activating solution to obtain a constant (initial water)/MK weight ratio of 0.78. Elaborated geopolymers formulations are reported in Tables 1 and 2.

Table 3. Physical and chemical characterization of Metakaolin by XRF, laser granulometry and N_2 adsorption-desorption (with BET method) as provided by the supplier.

Oxides	SiO_2	Al_2O_3	CaO	Fe_2O_3	TiO_2	K_2O
Composition %w/w	54.40	38.40	0.10	1.27	1.60	0.62
Granulometry (µm)	d_{10}	1.8	d_{50}	10.3	d_{90}	48.2
surface area (m^2/g)			18			

3.3. Acidity function measurements

Thiazole Yellow G (TYG, also known as Titan Yellow, Sigma-Aldrich) was used in the present study as the weak acid UV-visible-sensitive indicator, chosen to be compatible with the expected acidity function range of the studied solutions. Absorptions of activating solutions containing TYG were measured in the spectral range 300 to 600 nm, with a resolution of 1 nm, in 10-mm quartz cells at 25°C. Absorbance spectra were recorded on a dual-beam spectrophotometer (Genesys 10S UV-Visible, ThermoFischer Scientific), with a xenon flash lamp. Indicator-free activating solutions were used as backgrounds so that only the indicator would contribute to the recorded spectra. For the whole set of solutions, absorbance of indicator-free solutions was checked to be close to zero for wavelength ranging from 400 to 500 nm.

The absorbance at 480 nm has been checked to be proportional to TYG concentration up to approximately 5.10^{-4} mol / kg in sodium hydroxide solution, defining the range of validity of the Beer-Lambert law (details are available in supplementary information). Accordingly, the working concentration of TYG in all activating solutions was set to 5.10^{-5} mol / kg. In sodium hydroxide solutions, absorption bands centered at 405 and 475 nm have been observed respectively for the SH form and S^- form, with an isobestic point at 433 nm. In sodium silicate solution with increasing amounts of sodium hydroxide, absorption bands were centered at 390 and 480 nm, with an isobestic point at 438 nm. Previous observations from Allain and Xue[33] in sodium hydroxide solutions support the existence of a simple acid-base equilibrium for TYG as described in Reaction Equation 1. Allain and Xue also reported that TYG has a good chemical resistance to hydroxide ions, and a large dynamic spectral range. In addition, the similar position of the S^- form absorption band in both media corroborates the absence of any drastic conformation

modification, at least for the deprotonated form. This meant that silicates did not interact to any significant level with the indicator and that the latter was only involved in a simple acid-base equilibrium. Acidity functions were thus calculated from absorbance at 480 nm.

The pK_a of TYG has been measured in sodium hydroxide solution following Safavi and Abdollahi's procedure[34]. The pK_a value of 12.92 ± 0.01 at 25°C measured in this work is consistent with the 12.92 value reported by Safavi and Abdollahi. TYG was thus considered as a suitable weak acid indicator for acidity function measurements in study alkali silicate activating solutions.

Finally, the working range of TYG was established (see Sup. Inf.) to be comprised between 11.9 and 13.9, corresponding to an H_- range equal to approximately $pK_a \pm 1$, which is consistent with the dynamic spectral range found by Safavi and Abdollahi[34] and Allain and Xue[33].

3.4. Water activity measurements

Water activity was measured in all considered activating solutions in presence of 5.10^{-5} mol/L of TYG. Measurements were done at 25 ± 2°C with a Hygropalm HP23-AW-A analyzer equipped with a HC2-AW water activity probe (Rotronic) and calibrated in temperature and humidity with Rotronic certified humidity standards at 50% RH and 80% RH. After an equilibration time of 5 min, water activity was measured with a precision of ± 0.008. Water activity measurement relies on Equilibrium Relative Humidity measurement (ERH, in %), when the atmosphere in the sample holder is at equilibrium with the solution (a_{H2O} = ERH/100).

3.5. ^{29}Si Nuclear Magnetic Resonance.

^{29}Si NMR measurements were performed on silicate activating solutions to investigate the silicate connectivity. Spectra were recorded at a Larmor frequency of 99.36 MHz (at 25 ± 2°C) in zirconia rotors using a Bruker Avance spectrometer and a 7-mm commercial Bruker MAS probe but without spinning. 1600 transients were acquired using a single 90° pulse of 6.4 µs and a recycle time of 10 s. The recycle time was verified to be long enough by increasing it ten folds and confirming that intensities did not vary. Spectra were referenced externally to tetramethylsilane (TMS). The proportions of the different types of silicon centers were obtained by the integrated intensities of their resonances using the software Dmfit developed by D. Massiot *et al.*[35]. The different silicon centers were designated according to Engelhardt's nomenclature[15]. Each center is designated as Q since silicon atoms are quadri-coordinated to oxygen. A superscript Q^n ($0 \leq n \leq 4$) indicates the number of siloxo bonds (Si-O-Si), without considering the protonation degree of non-bridging oxygens. For example Q^0 designates a single silicate, Q^1 a silicate with one neighbor silicate (end-chain or in a dimer) and so on. When present, subscript c indicates that silicates are part of a three-membered ring. These Q^2 resonances are detected at slightly different frequencies compared to the ones of Q^2 groups in chains or larger rings due to their more constraint geometry.

3.6. Isothermal Conduction Calorimetry

Approximately 5 g of each elaborated geopolymer has been then introduced in a sealed ampoule to assess its reactivity by using Isothermal Conduction Calorimetry at 25°C on a TAM Air microcalorimeter. Water was used as the reference, to compensate for possible external temperature disturbances. Due to the external mixing procedure, a parasitic heat flow signal associated to the introduction of sample interfered with the initial reaction signal. The

equilibration time of this interference amounted to about 1.5 h, measured on an inert sample (available in supplementary information). Normalized heat flow release during geopolymerization, expressed in mW/g of paste, was recorded as a function of time during 90 h. Cumulative heat releases were obtained by integrating heat flow profiles after the end of the introduction peak here defined as when the heat flow drops to a value of 8 mW / g to minimize the contribution of the introduction peak.

4. Results

4.1. Acidity function H_- and alkalinity evaluation.

Acidity function values of were measured for the first time in sodium silicate solutions and compared to the ones of pure sodium hydroxide solutions. Results are plotted as a function of added sodium hydroxide molality in Figure 1.

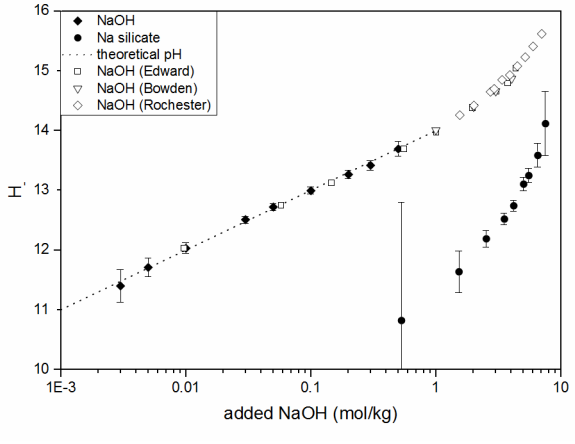

Figure 1. Comparison of H_- acidity function scales of pure sodium hydroxide (◆) or sodium silicate solutions (●) (with [Si] = 5.8 mol / kg) as a function of added sodium hydroxide molality. Literature data from Edward[29] (□), Bowden[30] (▽) and Rochester[32] (◇) were used for highly concentrated sodium hydroxide solutions. The dash line represents calculated theoretical pH which is equivalent to H_- in dilute solutions (< 1 mol / kg).

In a sodium hydroxide solution free from silicate, an addition of approximately 0.97 mol / kg sodium hydroxide is needed to raise the H_- value from 12.00 to 14.01 (value from Bowden[30]). Within this concentration range and in the specific case of pure sodium hydroxide solutions, H_- is fairly equivalent to theoretical pH calculated by $pK_w + log\ [OH^-]$ (with a mean deviation of 0.03) and our measured values were consistent with previously reported data[29]. Above 1 mol / kg, H_-

285 values are out of the working range of TYG, and cannot be measured with this indicator. For
286 sodium hydroxide addition higher than 1 mol / kg, the deviation of the H_- function from the
287 linearity is illustrated by plotting data from the literature[29,30,32]. Such a deviation is mainly due to
288 a sharp decrease in water activity as mentioned by Edward[29], which was measured for reference
289 and reported in Tables 1 and 2.
290 In a silicate-containing solution, an addition of approximately 4.0 mol / kg sodium hydroxide was
291 needed to raise the H_- value from 12.19 to 13.59. For higher sodium hydroxide additions, the
292 resulting H_- function values were higher than the 13.9 threshold value of TYG working range.
293 This set of data remarkably highlights the alkalinity difference between sodium hydroxide and
294 sodium silicate solutions. Alkalinity is here defined as the ability of a solution to resist changes in
295 pH in a given pH range. Using this working definition, the alkalinity of both sets of studied
296 solutions was calculated as the amount of hydroxide ions that has to be added to the solution to
297 raise the H_- value by one unit, within a H_- range from 12 to 14. For H_- values ranging from 12 to
298 14, the alkalinity values were found to be 0.48 mole added hydroxide per H_- unit for a silicate-
299 free solution and 2.86 for a solution containing 5.80 mol/kg of silicate,. Within the same acidity
300 function range, the alkalinity of the silicate-containing solution is thus more than 5 times higher
301 than the one of the silicate-free solution.
302

303 **4.2. Silicate connectivity**

304 Liquid state ^{29}Si NMR spectra of some sodium silicate solutions investigated herein are reported
305 on Figure 2. Several types of silicate species were present. The most deshielded are Q^0 silicates (δ
306 = -71.45 ppm in NaS1) and then Q^1 (δ = -79.45 ppm in NaS1), $Q^2{}_c$ (δ = -81.36 ppm in NaS1) Q^2
307 (δ = -87.47 ppm in NaS1), $Q^3{}_c$ (δ = -89.55 ppm in NaS1), Q^3 (i = -95.52 ppm in NaS1). A Q^4 (δ =

-105.4 ppm) resonance was only observed in NaS1. For indication, the ^{29}Si resonances are known to shift to higher frequencies (higher deshielding) when increasing the alkali hydroxide content. This well-known fact is due both to the deprotonation of silanol groups (Si-OH) and to the formation of ion pairs (Si-O^{-} $^{+}$Na) according to Kinrade and Swaddle[17]. As expected, when the alkali hydroxide content is increased, the peak intensities decreased for highly connected silicates and increases for poorly connected silicates, reflecting the general decondensation of silica oligomers with pH. Poorly resolved Q^2 and Q^3_c contributions were decomposed by fitting spectra with gausso-lorentzian lineshapes using the freeware Dmfit[35]. The average connectivity of Si centers was calculated from the spectral decomposition of ^{29}Si NMR measurements:

$$c = \frac{\sum_n n.Q^n}{\sum_n Q^n}$$

with Q^n the proportion of each silicate population (%).

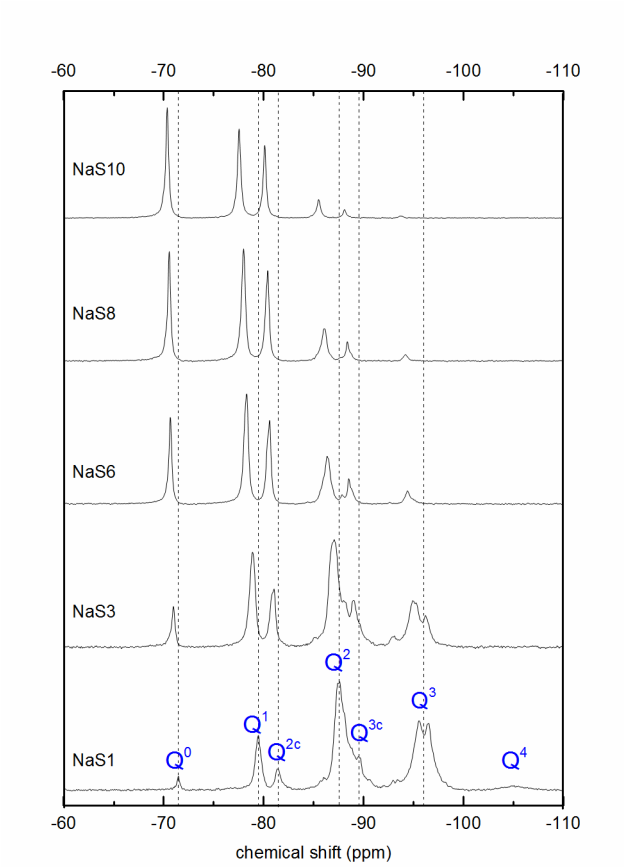

Figure 2. Liquid state ^{29}Si NMR spectra of some sodium silicate solutions investigated herein with varying sodium hydroxide contents. Peaks are named after Engelhardt notation[15].

On Figure 3, the average silicate connectivity is plotted as a function of acidity function values in silicate solutions. In the working range of TYG (dash lines), the average connectivity decreases for increasing *H*_ values. For sodium hydroxide additions from 2.54 to 6.54 mol/kg and corresponding *H*_ values ranging from 12.19 to 13.59 respectively, the silicate connectivity is divided by almost 2. It demonstrates the decondensation of silicates species when sodium hydroxide is added to solutions, as already reported by many authors.[15-17] Decondensation consists in the hydrolysis of siloxo bonds Si-O-Si. Such an effect, highlighted by Svensson *et*

al.[16], can be seen as the transfer of hydroxide ions from the solution onto silicates in the form of Si-OH groups. This leads to the consumption of initially added hydroxide ions, as illustrated by Reaction Equation 2:

$$(\equiv Si\text{-}O\text{-}Si\equiv)_{aq} + OH^- \leftrightarrow \equiv Si\text{-}OH + {}^-O\text{-}Si\equiv \qquad \text{(Reaction Equation 2)}$$

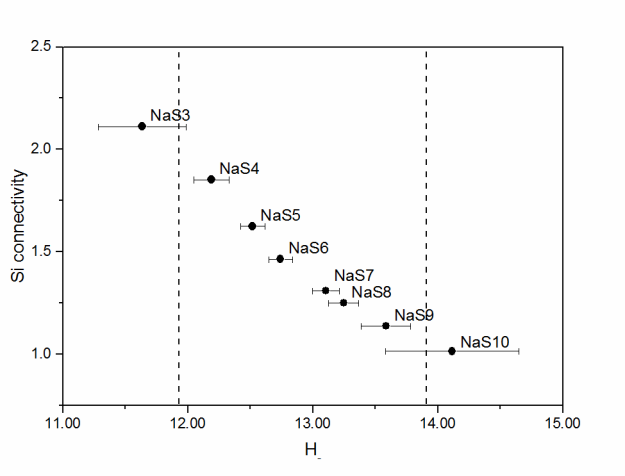

Figure 3. Evolution of the average connectivity of silicate oligomers in sodium silicate activating solutions as a function of their acidity function H- along the working range of the indicator TYG.

Consequently, it was apparent that the low *H*- values in silicate solutions (<14) despite their high sodium hydroxide contents, up to 7.5 mol/kg, were due to the presence of silicate species in solutions and to the associated reaction described above. The presence of silicate was thus responsible for the alkalinity measured in silicate-containing solutions.

4.3. Isothermal Conduction Calorimetry measurements

Metakaolin-based pastes were then prepared with the solutions under investigation. For all the studied compositions, cumulative heat profiles could be described as a succession of two stages[6-11] (Figure 4). The sharp heat release at the early beginning of the reaction can be ascribed mainly to the metakaolin dissolution. But this contribution often overlapped second stage of the

geopolymerization, namely the alumino-silicate polycondensation. After a variable duration, the heat release stabilized as the reaction slowed down. The heat value at the plateau (Figure 4 and 5) could then be assumed to be approximately proportional to the extent of geopolymerization.[6,9,10]

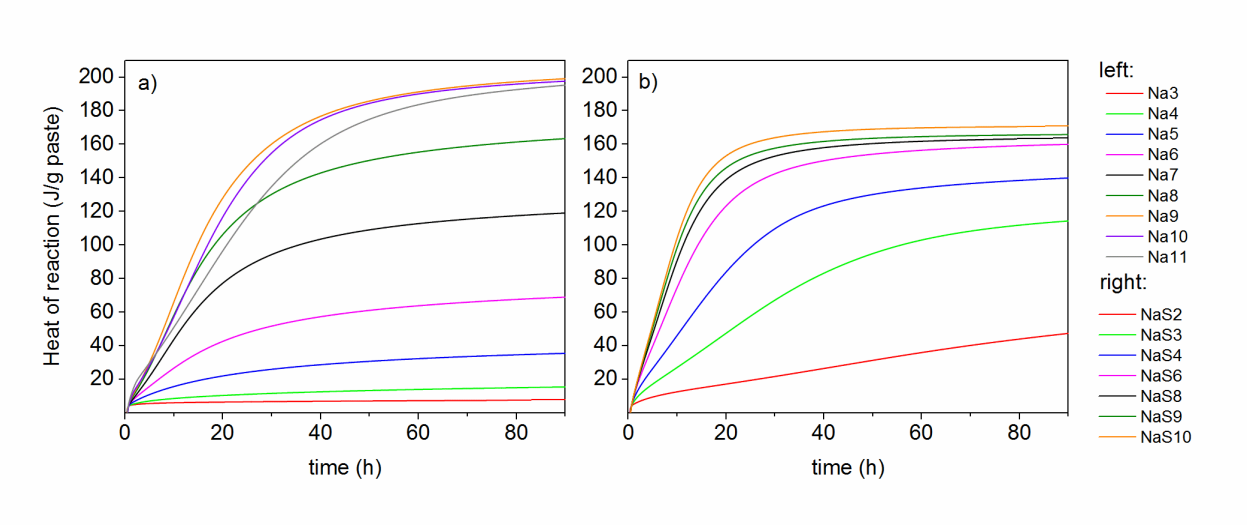

Figure 4. Total heat release of geopolymer pastes prepared from a) sodium hydroxide solutions and b) sodium silicate solutions, with varying NaOH content, measured by ICC.

5. Discussion

The final heat value was plotted as a function of total sodium ions content. In the same figure, the initial H_- values of the activating solutions were plotted on the right axis (Figure 5).

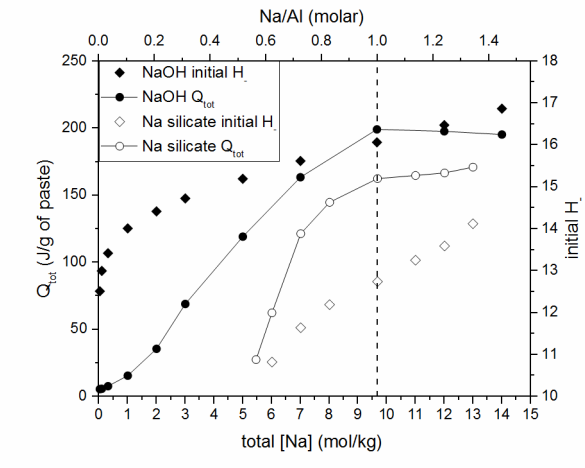

.

Figure 5. Comparison of the final heat released at 90 h of MK-based geopolymers measured by Isothermal Conduction Calorimetry (●) with the initial H_- function (◆) in either pure sodium hydroxide solutions (solid symbols) or sodium silicate solutions (empty symbols) as a function of total sodium molality.

For both sets of experiments, i. e. with or without silicate in the activating solution, increasing the total sodium ions molality by adding sodium hydroxide up to 9.66 mol / kg led to an increase in the heat of geopolymerization. Above this 9.66 mol / kg value, the heat released during geopolymerization remained constant. It has to be noted that this molality value corresponded to a Na/Al ratio equal to 1, described in literature[36] as the optimal geopolymer stoichiometry due to the charge balance between Na^+ ions and AlO_4^- units. At this point, the initial H_- values of activating solutions amount to 12.7 and 16.1 respectively in silicate-containing and silicate-free activating solution. At this 9.66 mol / kg sodium molality, (Na/Al = 1), the H_- value in the

371 silicate-containing solution was thus more than 3 units lower than in the silicate-free one. Despite
372 this huge difference, and for the same total sodium ions concentration, geopolymerization extents
373 were rather close in both systems.
374
375 While, it was predictable that the composition of the reactants with respects of the stoichiometry
376 of the final geopolymer product (Na/Al = 1) piloted the possibility or not to reach completion,
377 and that this explains the dependence on the sodium content of the activating solution, it
378 remained surprising at first glance that the silicate containing activating solutions, despite their
379 much lower initial *H*- values, led to large geopolymerization extent. Indeed, Xu and Van
380 Deventer[18] have demonstrated among others that increasing the pH value of the dissolution media
381 enhances alumino-silicate minerals dissolution and one might expect consequently a much lower
382 extent of reaction for metakaolin in silicate solutions than in pure NaOH ones. The benefits in
383 adding silicate species in activating solutions to enhance the geopolymerization process have
384 been previously mainly attributed to their role on condensation reactions, since silicate species
385 are available from the beginning of geopolymerization according to Duxson *et al.*[13]. Moreover,
386 Phair and Van Deventer[19] have shown that increasing the alkali content leads to less condensed
387 and more labile silicate species. A more porous and less dense geopolymer would thus be yielded
388 at lower modulus SiO_2/Na_2O[13,19].
389 However, the data presented here suggest another important role for the silicate species. When
390 using a silicate-free solution as the activating solution, hydroxide ions are consumed by
391 metakaolin dissolution, as described by Reaction Equation 3 as already reported by Xu and Van
392 Deventer[18]. Due to the low alkalinity of sodium hydroxide solutions, meaning, as defined in the

393 introduction, that they do not oppose pH changes, the pH necessarily drops during reaction and,
394 to insure that all metakaolin is dissolved, a high initial H_- value was necessary.
395
396 $(\equiv Si\text{-}O\text{-}(Si,Al)\equiv)_{metakaolin} + OH^- \leftrightarrow (\equiv Si\text{-}OH)_{metakaolin} + (\ ^-O\text{-}(Si,Al)\equiv)_{aq}$ (Reaction Equation 3)
397
398 At the opposite, when a silicate-containing solution was used to activate metakaolin and for a
399 same Na/Al ratio (typically 1), the H_- initial values were lower but a similar level of
400 geopolymerization was reached. Obviously, the lower acidity function H_- values were
401 compensated by the strong alkalinity resulting from the presence of silicate species. While
402 hydroxide ions are also consumed by the metakaolin dissolution which releases aluminate and
403 silicate species in solution, following Equation 3, the hydroxide are removed from solution but
404 the concomitant release of silicate and aluminate species in solution favors condensation of pre-
405 existing alumino-silicate species, thus releasing further hydroxide ions or water molecules in
406 solution (Reaction Equations 4 and 5). Those freshly released hydroxide ions are then available to
407 react in turn at the metakaolin surface, releasing more and more silicate and aluminate species
408 which can feed the condensation. As a result, a chain reaction can be established thanks to this
409 circular mechanism that nurtures the dissolution process. This phenomenon is enhanced in
410 silicate-containing solutions due to their alkalinity. In other terms, the initial silicate in solution
411 act as a reservoir of hydroxide compensating the effect of the H_- values which are initially lower
412 than in silicate-free solutions but remain probabbly somewhat constant during the dissolution.
413 $(\equiv Si\text{-}OH)_{aq} + (\ ^-O\text{-}(Si,Al)\equiv)_{aq} \leftrightarrow (\equiv Si\text{-}O\text{-}(Si,Al)\equiv)_{aq} + OH^-$ (Reaction Equation 4)
414 $(\equiv Si\text{-}OH)_{aq} + (HO\text{-}(Si,Al)\equiv)_{aq} \leftrightarrow (\equiv Si\text{-}O\text{-}(Si,Al)\equiv)_{aq} + H_2O$ (Reaction Equation 5)

It is understood, as shown in Reaction Equation 5, that condensation can also possibly release water molecules. Nevertheless, it has been shown that $Si(OH)_2O_2^{2-}$ and $Si(OH)_3O^-$ are the predominant forms of silicate monomers in activating solutions for geopolymers with respective pK_a's of 12.6 and 15.7[37]. Besides, silicates pK_a*'s* decrease with their connectivity[37]. In consequence, the level of silicate deprotonation should thus be significant in the present activating solutions. The release of hydroxide ions rather than water molecules would thus be favored.

5. Conclusion

Comparing initial H_- values at identical Na content in sodium hydroxide and sodium silicate allowed assessing for the first time the role of activating solution alkalinity in the geopolymerization process, where the alkalinity is defined as the ability of activating solutions to resist to H_- changes. As a consequence, the role of silicate species in the geopolymerization process is indirectly highlighted, since the presence of silicate species is responsible for activating solutions alkalinity.

The basicity of geopolymer activating solutions was investigated by UV-Visible spectroscopy using Thiazole Yellow G as a weakly acidic indicator to calculate their Hammett acidity function H_-. Sodium silicate and sodium hydroxide solutions alkalinity has thus been measured by using this methodology. The present results on sodium hydroxide solutions were consistent with previous results from Safavi[34], validating the implemented methodology. For the first time to our knowledge, this technique was applied to alkali silicate solutions. Quantitative data on the basicity of geopolymer activating solutions were obtained, without using pH-metry. Thiazole Yellow G was an appropriate indicator to measure H_- functions comprised in the range 11.9 - 13.9, which is ideally suitable for concentrated alkali silicate activating solutions.

438 The variation of acidity function was found low in silicate-based solutions when compared to
439 silicate-free solutions, for similar sodium hydroxide additions. This alkalinity difference, defined
440 as the ability of studied solutions to resist changes in pH, is due to the condensation and
441 decondensation of silicate species in the medium, as evidenced by using liquid state ^{29}Si NMR.
442
443 The reactivity of metakaolin-based geopolymers elaborated with previously investigated
444 activating solutions was studied by using Isothermal Conduction Calorimetry. Taking into
445 account initial H_- values and corresponding alkalinity of activating solutions allow to precise the
446 respective role of hydroxide ions and silicate species in the geopolymerization process. After
447 metakaolin dissolution initiation by hydroxide ions, the "hydroxide reservoir" on silicates can
448 gradually release hydroxide ions into the solution during the subsequent condensation of
449 alumino-silicate species. Those freshly released hydroxide ions would then be able to dissolve at
450 their turn additional amounts of metakaolin. This would generate a chain reaction and a self-
451 sustained circular mechanism. This high alkalinity explain why silicate solutions of low initial H_-
452 values lead to a similar extent of geopolymerisation compared to a silicate-free solution
453 presenting drastically higher H_- values. The fact that silicate solutions allow the reaction to take
454 place at lower hydroxide concentrations is probably crucial in directing the reaction path towards
455 geopolymers rather than zeolites.
456 Experimental work has to be enriched to further validate this proposition, especially by
457 measuring acidity functions during the course of geopolymerization. It must be understood
458 however that only discontinuous measurements would be possible with this technique, after
459 extracting the solution from the geopolymer paste at different times, since translucent media are
460 required for absorption based methods.

6. Conflicts of interest

There are no conflicts to declare

7. Reference section

(1) Davidovits, J. GEOPOLYMERS - Inorganic polymeric new materials. *J. Therm. Anal.* **1991,** *37* (8), 1633-1656.

(2) Duxson, P.; Fernandez-Jimenez, A.; Provis, J. L.; Lukey, G. C.; Palomo, A.; van Deventer, J. S. J. Geopolymer technology: the current state of the art. *J. Mater. Sci.* **2007,** *42* (9), 2917-2933.

(3) Provis, J. L.; Duxson, P.; van Deventer, J. S. J.; Lukey, G. C. The role of mathematical modelling and gel chemistry in advancing geopolymer technology. *Chem. Eng. Res. Des.* **2005,** *83* (A7), 853-860.

(4) Fernandez-Jimenez, A.; Palomo, A.; Criado, M. Microstructure development of alkali-activated fly ash cement: a descriptive model. *Cem. Concr. Res.* **2005,** *35* (6), 1204-1209.

(5) Khale, D.; Chaudhary, R. Mechanism of geopolymerization and factors influencing its development: a review. *J. Mater. Sci.* **2007,** *42* (3), 729-746.

(6) Buchwald, A.; Tatarin, R.; Stephan, D. Reaction progress of alkaline-activated metakaolin-ground granulated blast furnace slag blends. *J. Mater. Sci.* **2009,** *44* (20), 5609-5617.

(7) Granizo, M. L.; Blanco, M. T. Alkaline activation of metakaolin - An isothermal conduction calorimetry study. *J. Therm. Anal. Calorim.* **1998,** *52* (3), 957-965.

(8) Yao, X.; Zhang, Z. H.; Zhu, H. J.; Chen, Y. Geopolymerization process of alkali-metakaolinite characterized by isothermal calorimetry. *Thermochim. Acta* **2009,** *493* (1-2), 49-54.

(9) Zhang, Z. H.; Wang, H.; Provis, J. L.; Bullen, F.; Reid, A.; Zhu, Y. C. Quantitative kinetic and structural analysis of geopolymers. Part 1. The activation of metakaolin with sodium hydroxide. *Thermochim. Acta* **2012,** *539*, 23-33.

(10) Zhang, Z. H.; Provis, J. L.; Wang, H.; Bullen, F.; Reid, A. Quantitative kinetic and structural analysis of geopolymers. Part 2. Thermodynamics of sodium silicate activation of metakaolin. *Thermochim. Acta* **2013,** *565*, 163-171.

(11) Sun, Z. Q.; Vollpracht, A. Isothermal calorimetry and in-situ XRD study of the NaOH activated fly ash, metakaolin and slag. *Cem. Concr. Res.* **2018,** *103*, 110-122.

(12) Rahier, H.; Simons, W.; VanMele, B.; Biesemans, M. Low-temperature synthesized aluminosilicate glasses .3. Influence of the composition of the silicate solution on production, structure and properties. *J. Mater. Sci.* **1997,** *32* (9), 2237-2247.

(13) Duxson, P.; Provis, J. L.; Lukey, G. C.; Mallicoat, S. W.; Kriven, W. M.; van Deventer, J. S. J. Understanding the relationship between geopolymer composition, microstructure and mechanical properties. *Colloid Surf. A-Physicochem. Eng. Asp.* **2005,** *269* (1-3), 47-58.

(14) White, C. E.; Provis, J. L.; Proffen, T.; van Deventer, J. S. J. Molecular mechanisms responsible for the structural changes occurring during geopolymerization: Multiscale simulation. *Aiche J.* **2012,** *58* (7), 2241-2253.

(15) Engelhardt, G.; Zeigan, D.; Jancke, H.; Hoebbel, D.; Wieker, W. ^{29}Si NMR-Spectroscopy of Silicate Solutions .II. Dependence of Structure of Silicate Anions in Water Solutions from Na:Si Ratio. *Z. Anorg. Allg. Chem.* **1975,** *418* (1), 17-28.

(16) Svensson, I. L.; Sjoberg, S.; Ohman, L. O. Polysilicate Equilibria in Concentrated Sodium Silicate Solutions. *J. Chem. Soc., Faraday Trans. 1* **1986,** *82*, 3635-3646.

(17) Kinrade, S. D.; Swaddle, T. W. Silicon-29 NMR Studies of Aqueous Silicate Solutions .1. Chemical Shifts and Equilibria. *Inorg. Chem.* **1988,** *27* (23), 4253-4259.

(18) Xu, H.; Van Deventer, J. S. J. The geopolymerisation of alumino-silicate minerals. *Int. J. Miner. Process.* **2000,** *59* (3), 247-266.

(19) Phair, J. W.; Van Deventer, J. S. J. Effect of the silicate activator pH on the microstructural characteristics of waste-based geopolymers. *Int. J. Miner. Process.* **2002,** *66* (1-4), 121-143.

(20) Granizo, N.; Palomo, A.; Fernandez-Jimenez, A. Effect of temperature and alkaline concentration on metakaolin leaching kinetics. *Ceram. Int.* **2014,** *40* (7), 8975-8985.
(21) Drever, J. I. *The Geochemistry of Natural Water*. Pearson Education Canada: 1988.
(22) Flexser, L. A.; Hammett, L. P.; Dingwall, A. The Determination of Ionization by Ultraviolet Spectrophotometry: Its Validity and its Application to the Measurement of the Strength of Very Weak Bases. *J. Am. Chem. Soc.* **1935,** *57* (11), 2103-2115.
(23) Hammett, L. P.; Deyrup, A. J. A SERIES OF SIMPLE BASIC INDICATORS. I. THE ACIDITY FUNCTIONS OF MIXTURES OF SULFURIC AND PERCHLORIC ACIDS WITH WATER. *J. Am. Chem. Soc.* **1932,** *54* (7), 2721-2739.
(24) Hammett, L. P. THE THEORY OF ACIDITY. *J. Am. Chem. Soc.* **1928,** *50* (10), 2666-2673.
(25) Schwarzenbach, G.; Sulzberger, R. Über die Alkalinität starker Lösungen der Alkalihydroxyde. *Helv. Chim. Acta* **1944,** *27* (1), 348-362.
(26) Paul, M. A.; Long, F. A. H_0 AND RELATED INDICATOR ACIDITY FUNCTIONS. *Chem. Rev.* **1957,** *57* (1), 1-45.
(27) Stewart, R.; Odonnell, J. P. STRONGLY BASIC SYSTEMS .III. H_- FUNCTION FOR VARIOUS SOLVENT SYSTEMS. *Can. J. Chem.-Rev. Can. Chim.* **1964,** *42* (7), 1681-1693.
(28) Rochester, C. H. Correlation of Acidity Functions with Equilibria of p-Nitroaniline in Aqueous Sodium Hydroxide Solution. *Trans. Faraday Soc.* **1963,** *59* (492), 2820-2825.
(29) Edward, J. T.; Wang, I. C. IONIZATION OF ORGANIC COMPOUNDS .II. THIOACETAMIDE IN AQUEOUS SODIUM HYDROXIDE. THE H_- ACIDITY FUNCTION. *Can. J. Chem.-Rev. Can. Chim.* **1962,** *40* (3), 399-407.
(30) Bowden, K. ACIDITY FUNCTIONS FOR STRONGLY BASIC SOLUTIONS. *Chem. Rev.* **1966,** *66* (2), 119-131.
(31) Bandura, A. V.; Lvov, S. N. The ionization constant of water over wide ranges of temperature and density. *J. Phys. Chem. Ref. Data* **2006,** *35* (1), 15-30.
(32) Rochester, C. H. Correlation of Reaction Rates with Acidity Functions in Strongly Basic Media .Part 2. Reaction of 2,4-Dinitroaniline With Aqueous Sodium Hydroxide. *Trans. Faraday Soc.* **1963,** *59* (492), 2826-2837.
(33) Allain, L. R.; Xue, Z. L. Optical sensors for the determination of concentrated hydroxide. *Anal. Chem.* **2000,** *72* (5), 1078-1083.
(34) Safavi, A.; Abdollahi, H. Optical sensor for high pH values. *Anal. Chim. Acta* **1998,** *367* (1-3), 167-173.
(35) Massiot, D.; Fayon, F.; Capron, M.; King, I.; Calvé, S. L.; Alonso, B.; Durand, J. O.; Bujoli, B.; Gan, Z.; Hoatson, G. Modelling one- and two-dimensional solid-state NMR spectra. *Magn. Reson. Chem.* **2002,** *40* (1), 70-76.
(36) Rahier, H.; VanMele, B.; Biesemans, M.; Wastiels, J.; Wu, X. Low-temperature synthesized aluminosilicate glasses .1. Low-temperature reaction stoichiometry and structure of a model compound. *J. Mater. Sci.* **1996,** *31* (1), 71-79.
(37) Sefcik, J.; McCormick, A. V. Thermochemistry of aqueous silicate solution precursors to ceramics. *Aiche J.* **1997,** *43* (11), 2773-2784.